Polyvinylidene Fluoride (PVDF)/Modified Clay Hybrid Membrane for Humic Acid and Methylene Blue Filtration

Edi Pramono*, Gadis Prihatin Wahyu Sejati, Sayekti Wahyuningsih, and Candra Purnawan

Department of Chemistry, Faculty of Mathematics and Natural Sciences, Universitas Sebelas Maret, Jl. Ir. Sutami 36A, Kentingan, Surakarta 57126, Indonesia

** Corresponding author:*

email: edi.pramono.uns@staff.uns.ac.id

Received: November 7, 2022
Accepted: March 11, 2023

DOI: 10.22146/ijc.78979

Abstract: *This research studied the impact of silanized clay modification on performance and antifouling Poly(vinylidene fluoride) (PVDF) membrane toward humic acid and methylene blue filtration. Clay modification was carried out by using 3-aminopropyltriethoxysilane (APS) to produce modified clay (Clay-APS). Hybrid membranes were prepared by phase inversion for humic acid and methylene blue filtration. Hybrid membranes were characterized by measuring surface hydrophilicity, water flux, rejection, and antifouling properties. Clay and Clay-APS modification increased hybrid membrane surface hydrophilicity, as indicated by increasing the β fraction and decreasing the water contact angle. The PVDF/Clay and PVDF/Clay-APS hybrid membranes showed high permeability and selectivity with the highest water flux values of 24.2 L m^{-2} h^{-1}. The rejections for humic acid and methylene blue were 98.8 and 99.3%, respectively. The highest antifouling property was obtained from the PVDF/Clay-APS hybrid membrane, with a flux recovery ratio was 96.0%. The PVDF/Clay hybrid membrane performance and antifouling properties showed that the membranes have the potential for water treatment.*

Keywords: *clay modification; dye filtration; hybrid membrane; polyvinylidene fluoride*

■ INTRODUCTION

About 70% of the earth is water, but only 2.5% is a source of pure water and only 1% is fresh water accessible and used by 7.6 billion people [1]. Water sources in the tropics are mostly peat water, characterized by brownish-yellow water due to the high concentration of humic acid (HA) that cannot be consumed directly [2]. Therefore, peat water must be processed into clean water for daily needs, especially drinking water. In addition, clean water sources have also been significantly reduced with the development of industries that produce a lot of waste; as a result, more than 2 billion people have difficulty accessing clean water [3]. One produced waste is toxic dye waste, which can contaminate the soil, sediment, and surrounding surface water [4]. Wastewater treatment management is needed to balance water availability and demand at an affordable cost, which positively impacts the environment. Several technologies have been developed to address wastewater problems, such as adsorption, sedimentation, coagulation, biological treatment, photodegradation, and membrane filtration [5-6]. Membrane technology is a promising technique for removing impurities in water where the filtration efficiency is influenced by hydrophilicity properties and the porosity of the membrane surface [7].

Polymer membranes have greater flexibility, good film-forming properties, mechanical strength, chemical stability, and high selectivity [8]. In water treatment technology, membranes based on hydrophobic polymers have been widely applied such as polysulfone, poly(vinylidene fluoride) (PVDF), and polytetrafluoroethylene [9-10]. Hydrophobic polymers, including PVDF, have a disadvantage because the high hydrophobic surface properties can interact with foulants, causing fouling and reducing membrane performance [11]. Fouling mitigation has been developed using additives, hydrodynamic optimization, and membrane surface modification [12]. One way to

increase membrane efficiency and reduce fouling is to add hydrophilic compounds to the membrane [13]. Antifouling properties are measured as flux recovery ratio (FRR). Several previous studies reported that the addition of hydrophilic fillers such as PVDF-*g*-PDMAPMA, MWCNTs-OH, and TiO_2 could increase membrane FRR [14-16]. Another material that has the potential to modify PVDF membranes is clay. Various types of clay can be found in Indonesia, including bentonite, cloisite, and kaolinite [17]. Clay modification of PVDF membranes has been reported, such as the use of cloisite and halloysite [18-19]. Cosmetic-graded clay has non-toxic properties, hydrophilic, is easily obtained, and is inexpensive compared to other clays. However, studies on cosmetic clay application to PVDF membranes have not been reported yet.

Direct application of inorganic materials such as clay has an effect called agglomeration. It is caused by differences in surface tension between the polymer and fillers [20], the resulting membrane that can be inhomogeneous and difficult to cast. Surface modification by organosilane modification, such as 3-aminopropyltriethoxysilane (APS) could increase interaction between polymer and clays [21]. Preliminary tests of PVDF modification with kaolin clay have been carried out and showed an increase in membrane hydrophilicity. In this study, organosilane-modified clay (Clay-APS) and a PVDF/Clay-APS hybrid membrane were developed. The membrane was made using PVDF with a different molecular mass from previous studies [22]. This research investigated the effect of various concentrations of Clay-APS on membrane performance toward HA and methylene blue (MB) filtration; and also discussed surface characteristics as well as antifouling properties.

■ EXPERIMENTAL SECTION

Materials

The materials used in this study include PVDF (Mw 64.000 g/mol) was purchased from Jiangsu Freechem-China. *N*,*N*-dimethylformamide (DMF), polyethylene Glycol 400 (PEG400), hydrochloric Acid (HCl), and MB (Mw 319.85 g/mol) were purchased from Merck. APS was obtained from Sigma-Aldrich. HA was prepared by Edulab Indonesia. Clay cosmetic-based (containing kaolinite) was purchased from Cipta Kimia.

Instrumentation

The membranes were characterized using Attenuated Total Reflection Fourier Transform Infrared (ATR-FTIR Agilent 360) and Scanning Electron Microscopy (SEM, JEOL Benchtop JCM 7000). The dye solution concentration was analyzed using UV-Vis spectrophotometer (Hitachi UH5300).

Procedure

Modification of clay with APS

Clay was ground and sieved to size 200 mesh. The 4 g clay was soaked in 100 mL, HCl 0.1 M for 24 h and then dried at room temperature for 24 h. Modification of clay with APS followed previous research [23-25]. About 4 g of clay was dispersed in 200 mL of ethanol, then 4 g of APS, which had been dispersed into 50 mL ethanol. The mixture was stirred for 24 h at a temperature of 70 °C. The mixture was filtered and dried at 60 °C for 12 h. The modification has been successfully carried out and confirmed by FTIR spectra peak at 1568 cm^{-1}, which indicates the presence of an -NH group from APS, and at 2936 cm^{-1} which corresponds to a CH_2 of organosilane [26].

Membranes fabrication

PVDF and hybrid membranes were fabricated using the phase inversion following the previous report [27]. The casting solution (Dope) was carried out by various concentrations shown in Table 1. Clay or Clay-APS, PEG, and PVDF were mixed into DMF with a total mass of 9 g. The solution was stirred at 60 °C for 24 h. The dope was cast on glass with a thickness regulator of 130 μm and immediately put into a water bath as a coagulant bath. The obtained membrane was stored in glycerin and washed before being analyzed.

Characterization

The membranes were characterized by morphology, functional groups, contact angles, and pore

Table 1. Composition of 12 g dope solution

PVDF (wt.%)	PEG (wt.%)	Clay (wt.%)	Clay-APS (wt.%)	Membrane code
18	4	0	0	PVDF
18	4	1	0	PVDF/ Ka1
18	4	3	0	PVDF/Ka3
18	4	5	0	PVDF/Ka5
18	4	7	0	PVDF/Ka7
18	4	9	0	PVDF/Ka9
18	4	0	1	PVDF/Ka-APS1
18	4	0	3	PVDF/ Ka-APS3
18	4	0	5	PVDF/Ka-APS5
18	4	0	7	PVDF/Ka-APS7
18	4	0	9	PVDF/Ka-APS9

measurement. Membrane surface and cross-section morphology was analyzed by SEM. Functional group analysis on PVDF/Clay-APS hybrid membranes was carried out using the ATR-FTIR. Membranes were scanned 48 times at a range of 400–4000 cm^{-1} with a resolution of 4 cm^{-1}. The membrane polymorphs were computed using Eq. (1) [28],

$$F(\beta) = \frac{A\beta}{A\beta + 1.26A\alpha} \quad (1)$$

where F(β) is the relative fraction of the β phase, while Aα and Aβ are the absorbances at the peaks of 769 and 840 cm^{-1}, which correspond to the α and β phases, respectively.

Surface hydrophilicity was determined by measuring the membrane's water contact angle (WCA). A flat membrane was prepared on the sample holder and the water was dropped on the membrane's surface. The water drop image was recorded and processed using ImageJ software with a contact angle plugin.

Membrane porosity was analyzed using the gravimetric method. The wet membrane (W_b) was weighed and dried at 60 °C for 24 h. The dry membrane (W_k) was weighed again, and the membrane porosity (ε) was determined through Eq. (2),

$$\varepsilon(\%) = \left(\frac{W_b - W_k}{A \times l \times \rho} \right) \times 100 \quad (2)$$

where A is the area of the membrane, l is the thickness of the membrane, and ρ is the density of water.

Membrane performance test

The measurements were carried out using a microfiltration device as a stirred cell with a dead-end system. A membrane with a 5 cm diameter was attached to the sample holder. The system was operated under a transmembrane pressure (TMP) of 2 bar using 200 mL water as the feed phase. The membrane was compacted for 15 min and calculated the time to obtain 2 mL of permeate. The water flux was computed using Eq. (3),

$$J = \frac{V}{A \times t} \quad (3)$$

where J is the permeate flux ($L/m^2.h$), V is the volume of water permeate (L), A is the membrane surface area (m^2), and t is the measurement time (h).

The average membrane pore size can be calculated using the Geurout–Elford-Ferry formula at Eq. (4) [29],

$$r_p = \sqrt{\frac{(2.9 - 1.75\varepsilon) \times 8\rho \, lm \, Jw}{\varepsilon \times A \times \Delta P}} \quad (4)$$

where ε is membrane porosity (%), ρ is the deionized water viscosity at 25 °C (8.9×10^{-4} Pa s), lm is the wet membrane thickness, A is effective membranes surface, Jw is pure water flux, and ΔP is operating pressure (0.2 MPa).

The membrane rejection was measured by replacing the feed phase with HA and MB with a concentration of 100 mg L^{-1}. The structure of HA and MB are shown in Fig. 1 and 2 [30]. Permeate and retentate concentration was analyzed and the membrane rejection R(%) was calculated using Eq. (5). The antifouling was analyzed by calculating the value of the FRR in the form of a presentation between the membrane flux that had been used for filtration and the initial water flux. The values obtained from each repetition were then averaged. The FRR value is determined using Eq. (6).

$$R(\%) = \left(1 - \frac{C_p}{C_r} \right) \times 100\% \quad (5)$$

where C_p is the concentration of permeate and C_r is the retentate concentration.

$$FRR = \frac{J_n}{J_o} \times 100\% \quad (6)$$

where J_n is pure water flux after the rejection test and J_o is pure water flux before the rejection measurement.

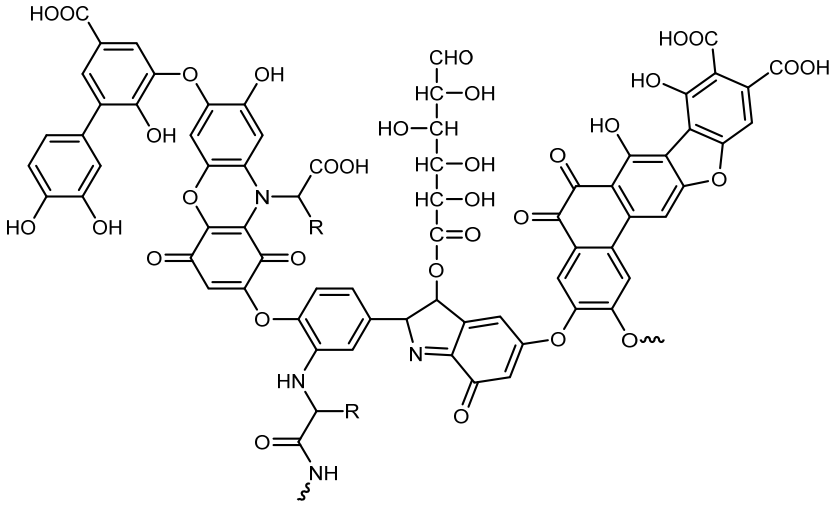

Fig 1. Hypothetic structure of humic acid [30]

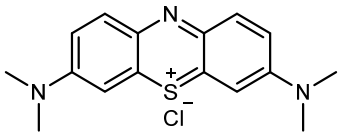

Fig 2. Chemical structure of methylene blue

■ RESULTS AND DISCUSSION

PVDF Membranes Polymorph

The polymorph of PVDF/Clay and PVDF/Clay-APS membranes were characterized by ATR-FTIR and presented in Fig. 3. The ATR-FTIR spectra in Fig. 3(a) obtained the peaks at 769 and 840 cm^{-1}, corresponding to the vibration of C-H and C-F with different conformations. The peaks at 769 and 840 cm^{-1} were related to the α and β phases, respectively. The α phase has the non-polar TGTG' conformation and the β phase has the most polar nature with the TTTT' conformation. Fig. 3 also shows the change in the value of the β fraction on the membrane. Fig. 3(b) showed the β fraction of the pristine PVDF membrane of 0.47, and the addition of clay and Clay-APS to the PVDF membrane caused increasing in the β fraction. The increasing β phase of PVDF/Clay membranes is linear with the amount of clay added, indicating an increase in the hydrophilicity of the membrane because the β phase showed the polar nature of the PVDF [31]. The β fraction of PVDF/clay APS membranes is relatively constant in Clay-APS concentration up to 3%, and it is caused by the existence of a silane group from APS that tend to have hydrophobic property.

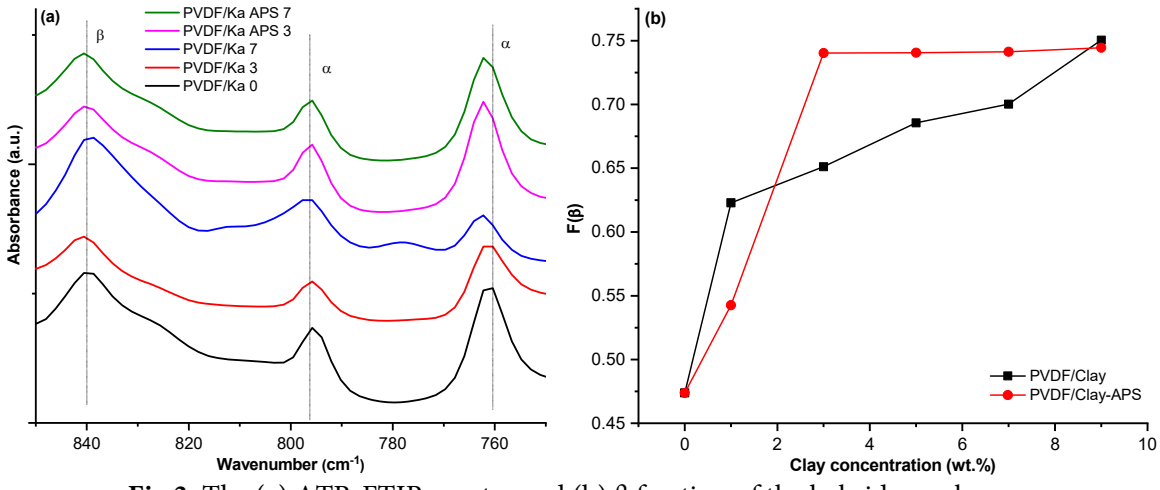

Fig 3. The (a) ATR-FTIR spectra and (b) β fraction of the hybrid membranes

Membrane Surface Hydrophilicity

Membrane surface hydrophilicity was analyzed by WCA and given in Fig. 4. The pristine membrane obtained a WCA of 85.6°, which indicates that the membrane is relatively hydrophilic. Fig. 4 also showed decreasing WCA after PVDF/Clay and PVDF/Clay-APS modification. A considerable decrease in the contact angle occurs after the addition of clay with a concentration of 3 wt.% where the value is below 75 °C, and it reaches below 70 °C at the addition of 9 wt.% concentration. The clay and Clay-APS modified membranes are more hydrophilic due to the existence of Clay and the increasing of β fraction.

The image of water droplets on the membrane at various observation times is shown in Fig. 5. The water contact angle decreased with aging time, and the dimensions of the water droplets presented that there was no diameter widening. The dynamic contact angle reduction of PVDF/Clay 3% and PVDF/Clay-APS 7% in Fig. 6 were observed faster than the pristine membrane and almost reached 20 °C for 12 min. The decrease in contact angle on the membrane surface can be influenced by surface hydrophilicity and pore properties. Decreasing the water droplet contact angle without a change of diameter indicated that it is dominantly caused

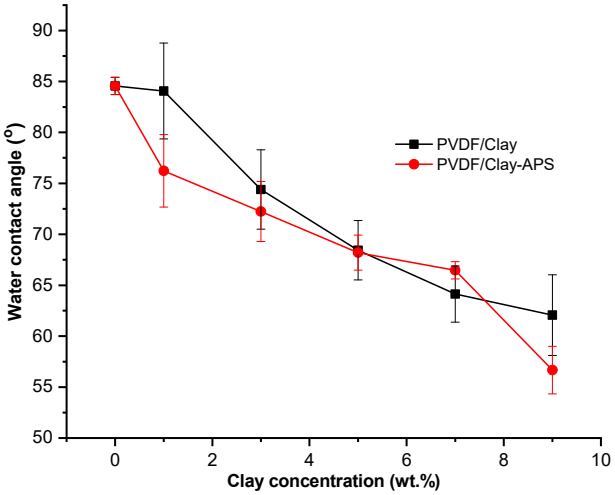

Fig 4. WCA of PVDF/Clay and PVDF/Clay-APS hybrid membranes

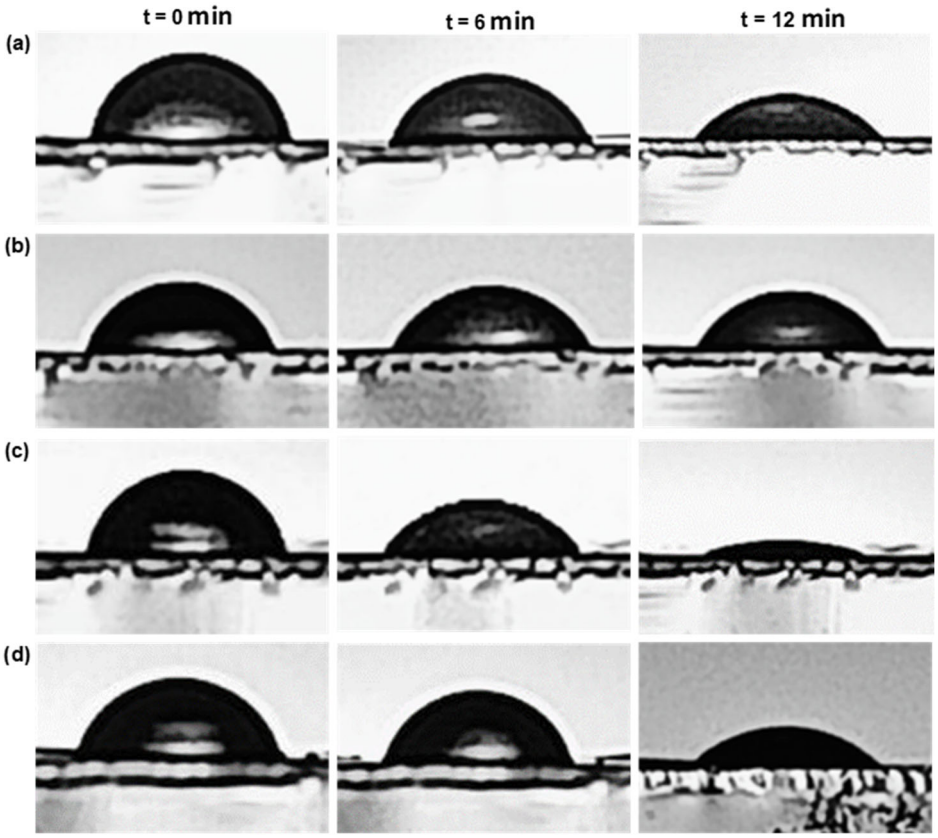

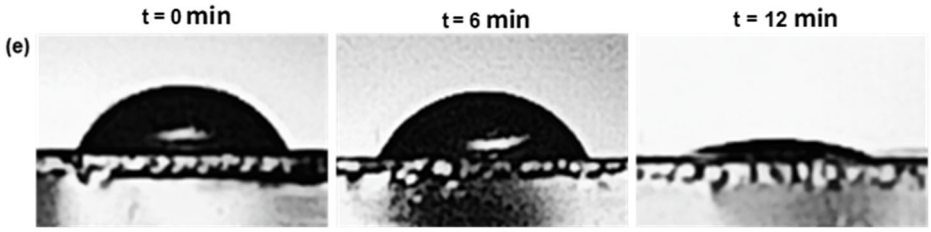

Fig 5. Water droplet aging on (a) PVDF;(b) PVDF/Ka 3%; (c) PVDF/Ka 7%; (d) PVDF/Ka-APS; (e) PVDF/Ka-APS 7 wt.% membrane surface

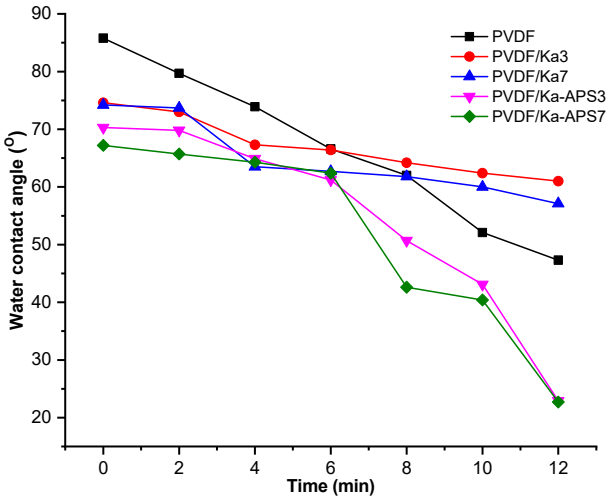

Fig 6. The dynamic water contact angle of hybrid membranes

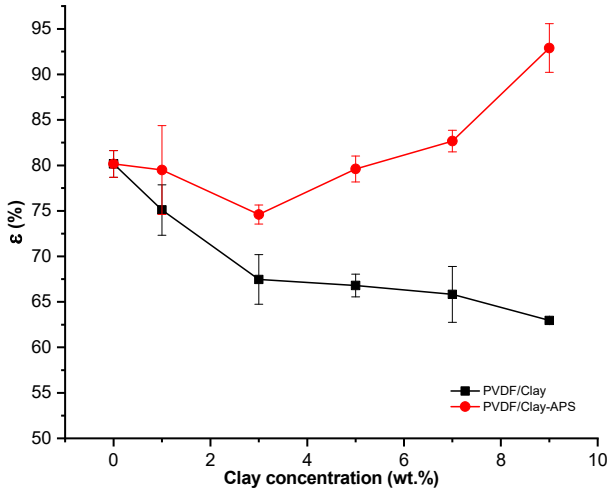

Fig 7. The porosity of PVDF/Clay and PVDF/Clay-APS hybrid membranes

by the pores in the membrane. The decline of water contact angle is in accordance with previous research [32] which shows that the pore factor can cause changes in contact angle.

Membrane Porosity

Membrane porosity measurement was carried out using the gravimetric method and data presented in Fig. 7. The porosity of the pristine PVDF membrane has a high value of 80.2% and decreases with clay addition. On the other hand, the additional high concentration of clay APS increases membrane porosity. Membrane porosity is influenced by the presence of PEG as a porogen in dope. PEG can increase the number of pores and the pore area [33]. PEG, a hydrophilic substance, will be pulled out during the phase inversion due to the interaction with the water coagulant and leave pores in the membrane. The addition of clay can hinder water and PEG during the phase inversion [34], which impacts the exchange solvent-non-solvent, resulting in lower porosity of the hybrid membrane. There is a probability that the presence of APS causes a different trend of porosity values in the PVDF/Clay-APS membrane. The existence of APS influences the membrane to be more hydrophobic; it affects the lower interaction with PEG and causes PEG to be easy to release during phase inversion.

Membrane's Morphology

Membrane surface and cross-section morphology are shown in Fig. 8. Based on surface morphology, PVDF and hybrid membranes had relatively the same surface, i.e., dense and rough. The cross-section of the membrane showed an asymmetric structure and consisted of macro and micropores. As described in the previous section, these pores form when PEG is released from the polymer component during phase inversion, resulting in membrane pores [35]. Fig. 8 shows the micro and macropore dimensions differences between PVDF

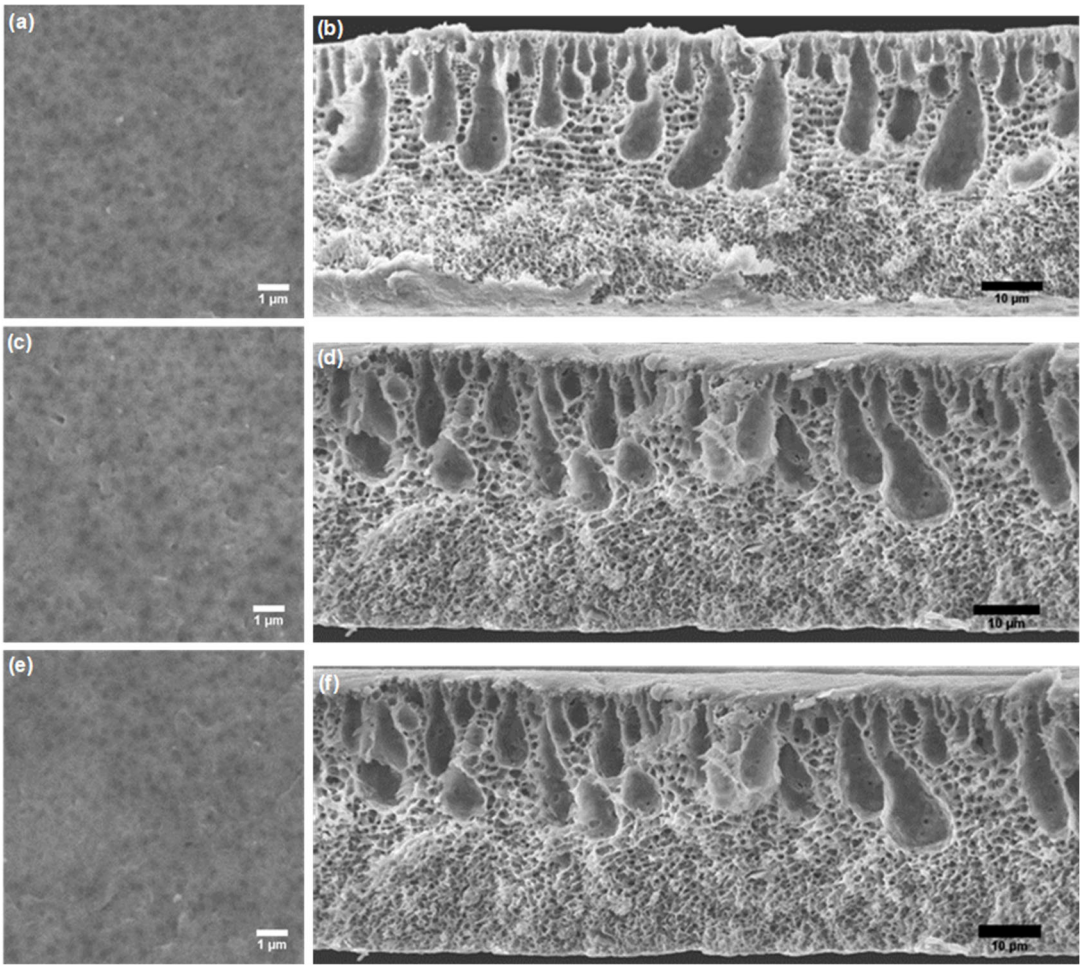

Fig 8. Surface and cross-section image of (a, b) PVDF; (c, d) PVDF/Clay 3%; (e, f) PVDF/Clay-APS 3 wt.%

and hybrid membranes. PVDF membrane produced a higher macropore but a smaller micropore on the bottom side. PVDF/Clay 3% and PVDF/Clay-APS 3% membranes showed a bigger micropore than the PVDF membrane. PVDF membrane had the lowest PWF because the micropore size was smaller, and PVDF/Clay 3% membrane had the highest flux due to the existence of macropore and high micropore.

Pure Water Flux and Pore Size of Membranes

Based on Fig. 9, the pure water flux (PWF) and pore size clay-modified membranes decreased with increasing clay concentration. This result was in line with the porosity data. The PWF increased by 1 and 3 wt.% Clay-APS addition. It could be due to the effect of APS as a modifier on the clay, which can increase the homogeneity of the membrane so that the obtained water flux can also increase until it reaches a maximum concentration of 3 wt.%. PVDF/Clay 3% and PVDF/Clay-APS 3% have high PWF due to the existence of micropores. It was linear with morphology data. In contrast, higher concentration addition of Clay-APS decreased PWF. Higher clay concentration can induce agglomeration [36] and pore filling by clay substrate, making the membrane pores denser.

Performance of PVDF/Clay Membrane for HA Filtration

The membrane's performance on HA was analyzed by the water flux and its rejection. Fig. 10 shows that the water flux of the pristine PVDF membrane with HA as a feed obtained a lower value than pure water flux. The presence of HA results in interactions on the surface and closure of pores in the membrane, which results in a

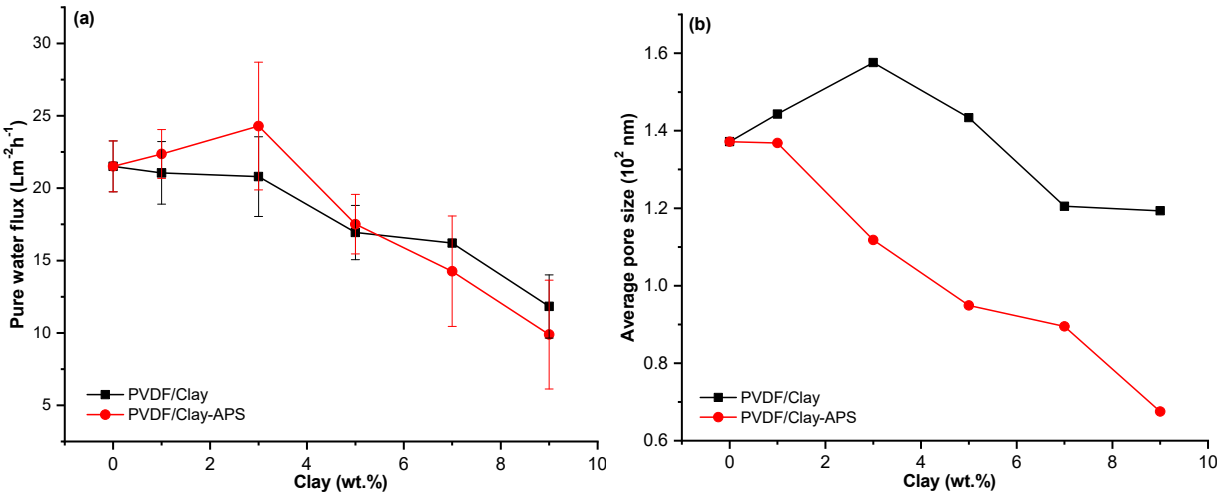

Fig 9. The (a) Pure water flux and (b) Average pore size of PVDF/Clay and PVDF/Clay-APS hybrid membranes

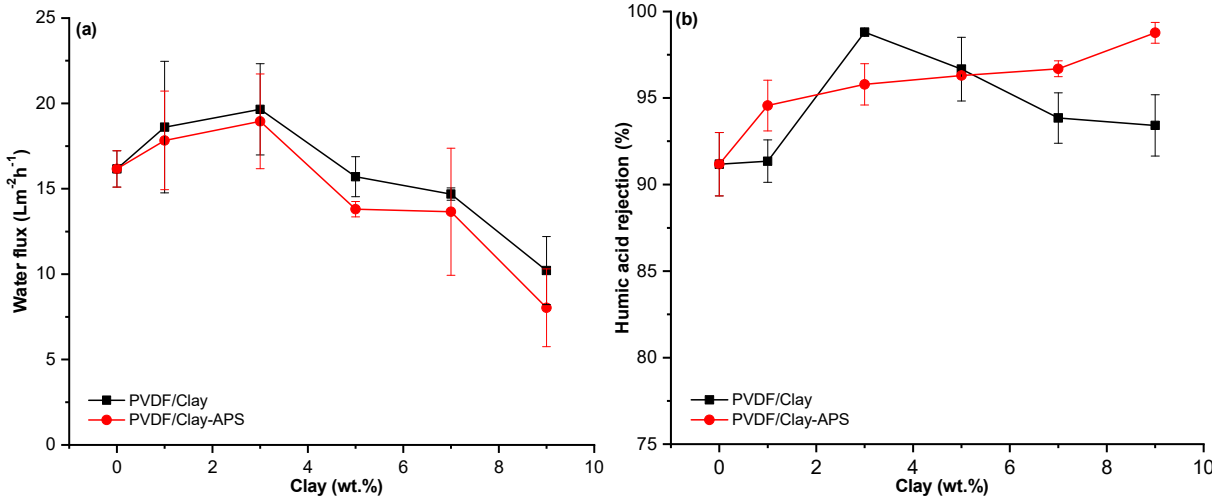

Fig 10. Performance of: (a) Water permeability and (b) Selectivity of PVDF/Clay and PVDF/Clay-APS membranes on HA filtration

decrease in membrane permeability. The PVDF/Ka3 and PVDF/KaAPS3 membranes showed the optimum water flux, where the flux value almost reaches 20 L m^{-2} h^{-1}. On the other hand, adding a higher clay concentration causes the flux value to decrease considerably due to the possibility of agglomeration. These results are linear with the porosity and pore size of the membrane.

HA rejection was obtained above 90.0%, which indicates that PVDF and PVDF/clays hybrid membranes were acceptable for water treatment. The 3 wt.% addition increased the membrane rejection and water flux, where the %R was up to 98.8%. The membrane rejection decreased at the clay addition of 5 to 9 wt.%, which could be caused by a larger pore size than the HA particle size. High clay content resulted in repulsion between the clay particles and the polymer and induced larger pores formation in the membrane cross-section. The PVDF/Clay-APS membrane showed an increase in the rejection value with the increase in filler concentration. The highest %R was reached at 9 wt.% Clay-APS addition of 98.0%. The linear enhancement of rejection percentage showed that the modification of Clay-APS in the membrane solution had a good effect on the membrane homogeneity.

Performance of PVDF/Clay Membranes for MB Filtration

The membrane filtration performance was also carried out on the filtration of MBdye, and the results were presented in Fig. 11. The modification of clay and Clay-APS to the PVDF membrane demonstrated a high %R of more than 90.0% and increased until %R of 99.1% for 3 wt.% addition. The water flux of the PVDF/Clay membrane in MB filtration had almost the same pattern as the water flux in HA filtration, where the water flux decreased. The PVDF/Clay-APS membrane produced a lower flux than the PVDF/Clay membrane and obtained less than 10 L m^{-2} h^{-1}. The overall %R value for MB was higher than HA. MB particles tend to interact with the clay-containing membrane surface so that it will be left in the feed phase.

The PVDF/Clay-APS membrane showed an increase in the rejection with increasing filler concentration up to 99.3% for PVDF/Clay-APS 3%. Membrane rejection PVDF/Clay-APS showed a value that tended to be constant at the addition of Clay-APS concentration above 3 wt.%, but the PVDF/Clay-APS 9% membrane had the highest rejection value of 99.5%. The water flux value of the PVDF/Ka-APS membrane was lower than clay-modified membranes, which results in a higher rejection value because the flux value is inversely proportional to the rejection value. The dye filtration was influenced by the pores' properties and the membrane's interaction with the dye. MB particles in solution can form molecular aggregations [37], produce large molecular dimensions, and cannot pass through the membrane pores. The interaction of negative charge on clay and cationic dyes also causes MB to be retained longer on the membrane surface, resulting in a high %R.

Membrane Antifouling Properties

Antifouling membrane properties were determined by calculating the FRR value for both HA and MB, and the results are given in Fig. 12. Pristine PVDF membrane obtained FRR of less than 80.0% toward HA filtration, indicating that water permeation decreased by about 20.0% after HA filtration. Decreasing water flux after feed filtration was related to fouling on the membrane surface [38-39]. The FRR value of the PVDF/clay membrane increased dramatically with the addition of 3 wt.%, where the value exceeded 90.0%. Membranes with the addition of clay and Clay-APS 3–7 wt.% had FRR relatively same, but there was an increase in FRR for Clay 9% and Clay-APS 9 wt.% contained membranes where the value exceeded 95.0% for HA and MB filtration.

Fig. 12 also revealed that the FRR value of the hybrid PVDF membrane for MB filtration was obtained lower than the FRR value for HA filtration. The FRR value on the membrane increased due to the increase in hydrophilicity, which is in accordance with the contact angle data. Membranes with hydrophilic surfaces will

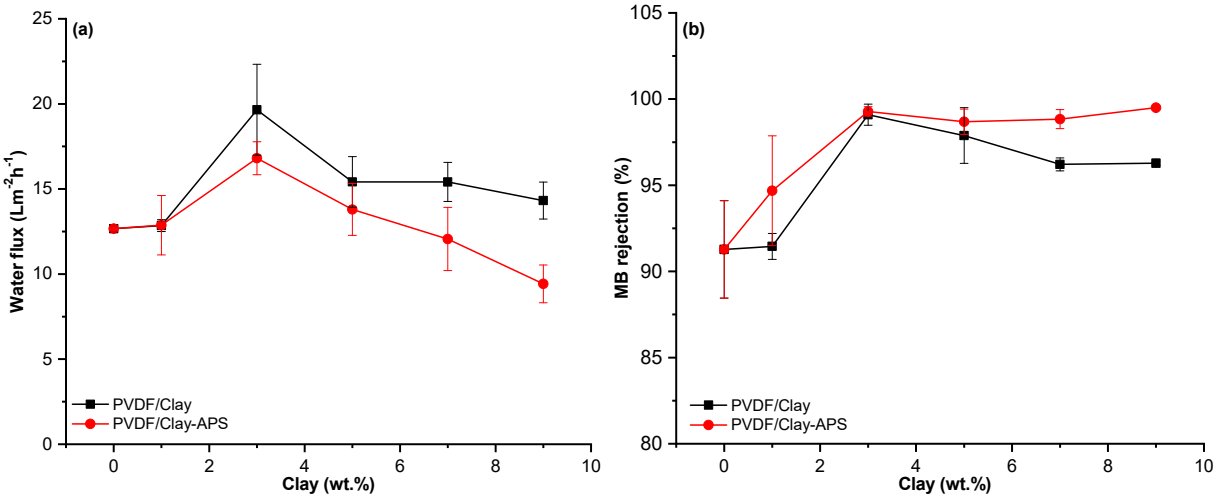

Fig 11. Performance of (a) water permeability and (b) selectivity of PVDF/Clay and PVDF/Clay-APS membranes on MB filtration

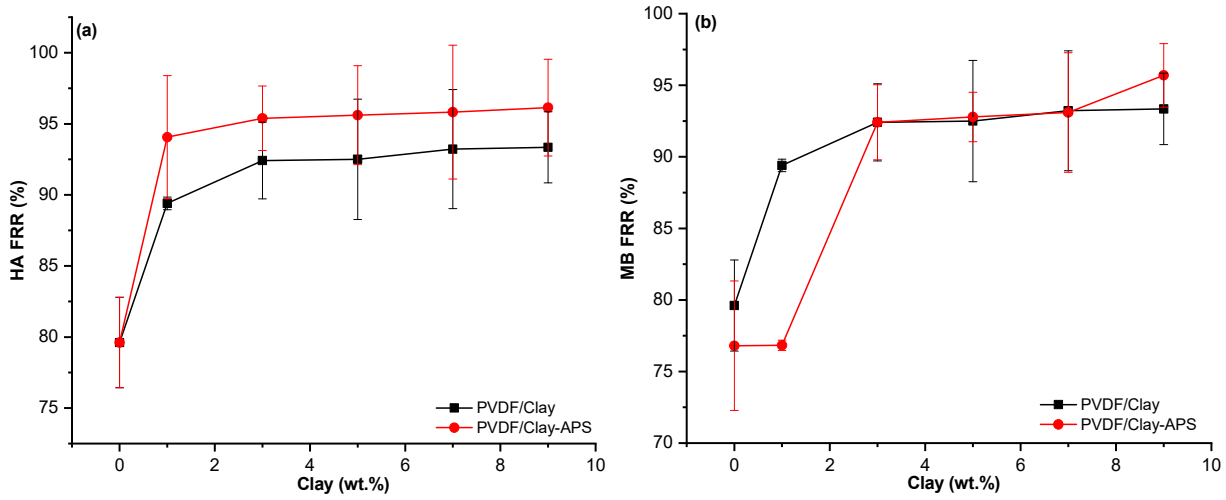

Fig 12. FRR of (a) HA and (b) MB filtration

Table 2. Comparative study of modified PVDF membranes for water treatment

Matrix	Type of membrane	Pure water flux ($L\ m^{-2}\ h^{-1}$)	Feed solution (Concentration)	Rejection (%)	FRR (%)	References
PVDF/Clay-APS	Micro filtration	24.3	MB (100 mg L^{-1})	99.3	92.4	This study
PVDF/Clay	Micro filtration	20.8	HA (100 mg L^{-1})	98.8	92.4	This study
PVDF/NZP	Ultra filtration	730.0	HA (20 mg L^{-1})	80.0	100.0	[43]
TP/PEI/PVDF	Ultra filtration	140.0	MB (20 mg L^{-1})	95.2	84.6	[44]
PVDF/Fe_3O_4-HNTs	Nano filtration	24.2	MB (100 mg L^{-1})	84.7	-	[45]
PVDF/GO-Ni	Ultra filtration	38.4	CR (50 mg L^{-1})	98.0	-	[46]

form a layer of pure water on the surface, which can prevent the adsorption and deposition of hydrophobic [40]. Antifouling properties were also supported by ATR-FTIR data which showed an increase in the β phase of the hybrid membrane. Based on the "Polar spreads on Polar" rule, the wettability of PVDF membranes could change according to the polarity of the crystalline phase, which affected membrane antifouling properties [41]. Conventional PVDF membranes generally contain a lot of non-polar phases and induced fouling due to high adhesive interactions between the foulant and the membrane surface. The presence of clay in the PVDF membrane influenced the strong interaction between the dye and membrane surface. Generally, clays particle were negatively charged and encouraged interactions with cationic molecules [42]. These resulted in a lower FRR of MB than HA for both PVDF and hybrid membranes.

PVDF/Clay and PVDF/Clay-APS membrane's performance shows the potential for water treatment applications. The results of the water flux, rejection, and antifouling of membranes are quite high compared to several previous studies on modified PVDF membranes for water treatment, as shown in Table 2. The membrane flux value is not too high but produces a high rejection, which is more than 98.0% for HA. The rejection value of the PVDF/Clay-APS membrane on MB dye was 99.0%, also quite high compared to the rejection value of other modified PVDF membranes. The FRR value produced on PVDF/Clay and PVDF/Clay-APS membranes was > 90.0%, showing good antifouling properties compared with other modified PVDF membranes.

■ CONCLUSION

PVDF and clay-modified hybrid membranes were successfully fabricated using phase inversion and produced asymmetric membranes with micro and macropore. Clay and Clay-APS addition could increase the membrane surface's hydrophilicity. The presence of

clay decreased membrane porosity and reversely for Clay-APS addition. The membrane's selectivity increased with the addition of Clay and Clay-APS. The most effective membrane for HA filtration is PVDF/Clay-APS 3% with water flux of 18 L m^{-2} h^{-1}, rejection of 96.0%, and FRR above 95.0%. Meanwhile, the most effective membrane for MB filtration is PVDF/Clay 3% with a water flux of 20 L m^{-2} h^{-1}, rejection of 99.1%, and FRR above 92.0%. These indicate that PVDF/Clay and PVDF/Clay-APS membranes can be applied in industrial applications, especially at HA and dye filtration.

■ ACKNOWLEDGMENTS

The author(s) would like to acknowledge LPPM UNS for providing financial support through a fundamental research grant No. 254/UN27.22/PT.01.03/2022.

■ AUTHOR CONTRIBUTIONS

Edi Pramono conducted data analysis, supervised the experiment, and wrote the manuscript. Gadis Prihatin Wahyu Sejati prepared a hybrid membrane and analyzed the membrane's performance. Sayekti Wahyuningsih and Candra Purnawan review the manuscript. All authors agreed to the final version of this manuscript.

■ REFERENCES

[1] Yalcinkaya, F., Boyraz, E., Maryska, J., and Kucerova, K., 2020, A review on membrane technology and chemical surface modification for the oily wastewater treatment, *Materials*, 13 (2), 493.

[2] Aryanti, P.T.P., Noviyani, A.M., Kurnia, M.F., Rahayu, D.A., and Nisa, A.Z., 2018, Modified polysulfone ultrafiltration membrane for humic acid removal during peat water treatment, *IOP Conf. Ser.: Mater. Sci. Eng.*, 288, 012118.

[3] Lin, F., Zhang, S., Ma, G., Qiu, L., and Sun, H., 2018, Application of ceramic membrane in water and wastewater treatment, *E3S Web Conf.*, 53, 04032

[4] Yaseen, D.A., and Scholz, M., 2019, Textile dye wastewater characteristics and constituents of synthetic effluents: A critical review, *Int. J. Environ. Sci. Technol.*, 16 (2), 1193–1226.

[5] Muneeb, M., Ismail, B., Fazal, T., Khan, R.A., Khan, A.M., Bilal, M., Muhammad, B., and Khan, A.R., 2018, Water treatment by photodegradation on orthorhombic antimony sulfide powder and effect of key operational parameters using methyl orange as a model pollutant, *Arabian J. Chem.*, 11 (7), 1117–1125.

[6] Xu, L., Shan, B., Gao, C., and Xu, J., 2020, Multifunctional thin-film nanocomposite membranes comprising covalent organic nanosheets with high crystallinity for efficient reverse osmosis desalination, *J. Membr. Sci.*, 593, 117398.

[7] Gopakumar, D.A., Arumukhan, V., Gelamo, R., Pasquini, D., de Morais, L.C., Rizal, S., Hermawan, D., Nzihou, A., and Khalil, H.P.S.A., 2019, Carbon dioxide plasma treated PVDF electrospun membrane for the removal of crystal violet dyes and iron oxide nanoparticles from water, *Nano-Struct. Nano-Objects*, 18, 100268.

[8] Brunetti, A., Tocci, E., Cersosimo, M., Kim, J.S., Lee, W.H., Seong, J.G., Lee, Y.M., Drioli, E., and Barbieri, G., 2019, Mutual influence of mixed-gas permeation in thermally rearranged poly(benzoxazole-co-imide) polymer membranes, *J. Membr. Sci.*, 580, 202–213.

[9] Shen, Z., Chen, W., Xu, H., Yang, W., Kong, Q., Wang, A., Ding, M., and Shang, J., 2019, Fabrication of a novel antifouling polysulfone membrane with in situ embedment of MXene nanosheets, *Int. J. Environ. Res. Public Health*, 16 (23), 4659.

[10] Mat Nawi, N.I., Chean, H.M., Shamsuddin, N., Bilad, M.R., Narkkun, T., Faungnawakij, K., and Khan, A.L., 2020, Development of hydrophilic PVDF membrane using vapour induced phase separation method for produced water treatment, *Membranes*, 10 (6), 121.

[11] Goh, P.S., Lau, W.J., Othman, M.H.D., and Ismail, A.F., 2018, Membrane fouling in desalination and its mitigation strategies, *Desalination*, 425, 130–155.

[12] Arumugham, T., Kaleekkal, N.J., Rana, D., and Doraiswamy, M., 2016, Separation of oil/water emulsions using nano MgO anchored hybrid ultrafiltration membranes for environmental abatement, *J. Appl. Polym. Sci.*, 133 (1), 42848.

[13] Kang, G., and Cao, Y., 2014, Application and modification of poly(vinylidene fluoride) (PVDF) membranes – A review, *J. Membr. Sci.*, 463, 145–165.

[14] Liu, L., Huang, L., Shi, M., Li, W., and Xing, W., 2019, Amphiphilic PVDF-*g*-PDMAPMA ultrafiltration membrane with enhanced hydrophilicity and antifouling properties, *J. Appl. Polym. Sci.*, 136 (42), 48049.

[15] Wang, W., Xu, X., Zhang, Z., Zhang, P., Shi, Y., and Ding, P., 2021, Study on the improvement of PVDF flat ultrafiltration membrane with MWCNTs-OH as the additive and the influence of different MWCNTs-OH scales, *Colloid Interface Sci. Commun.*, 43, 100433.

[16] Deng, W., Fan, T., and Li, Y., 2021, In situ biomineralization-constructed superhydrophilic and underwater superoleophobic PVDF-TiO_2 membranes for superior antifouling separation of oil-in-water emulsions, *J. Membr. Sci.*, 622, 119030.

[17] Gonggo, S.T., Edyanti, F., and Suherman, S., 2013, Karakterisasi fisikokimia mineral lempung sebagai bahan dasar industri keramik di desa Lembah Bomban kecamatan Bolano Lambunu kabupaten Parigi Moutong, *JAK*, 2 (2), 105–113.

[18] Wae AbdulKadir, W.A.F., Ahmad, A.L., and Ooi, B.S., 2021, A water-repellent PVDF-HNT membrane for high and low concentrations of oxytetracycline treatment via DCMD: An experimental investigation, *Chem. Eng. J.*, 422, 129644.

[19] Farahani, M.H.D.A., and Vatanpour, V., 2018, A comprehensive study on the performance and antifouling enhancement of the PVDF mixed matrix membranes by embedding different nanoparticulates: Clay, functionalized carbon nanotube, SiO_2 and TiO_2, *Sep. Purif. Technol.*, 197, 372–381.

[20] Ravi, J., Othman, M.H.D., Matsuura, T., Ro'il Bilad, M., El-badawy, T.H., Aziz, F., Ismail, A.F., Rahman, M.A., and Jaafar, J., 2020, Polymeric membranes for desalination using membrane distillation: A review, *Desalination*, 490, 114530.

[21] Ondrušová, D., Božeková, S., Buňová, L., Pajtášová, M., Labaj, I., Dubec, A., and Vršková, J., 2018, Modification of alternative additives and their effect on the rubber properties, *MATEC Web Conf.*, 157, 07007.

[22] Ismoyo, Y.A., Sejati, G.P.W., Pranoto, P., and Pramono, E., 2022, The potential of polyvinylidene fluoride (PVDF)-kaolin membrane for water treatment, *J. Phys.: Conf. Ser.*, 2190, 012022.

[23] de Souza Lima, J., Costa, F.N., Bastistella, M.A., de Araújo, P.H.H., and de Oliveira, D., 2019, Functionalized kaolin as support for endoglucanase immobilization, *Bioprocess Biosyst. Eng.*, 42 (7), 1165–1173.

[24] Mbaye, A., Diop, C.A.K., Miehe-Brendle, J., Senocq, F., and Maury, F., 2014, Characterization of natural and chemically modified kaolinite from Mako (Senegal) to remove lead from aqueous solutions, *Clay Miner.*, 49 (4), 527–539.

[25] Tao, Q., Su, L., Frost, R.L., Zhang, D., Chen, M., Shen, W., and He, H., 2014, Silylation of mechanically ground kaolinite, *Clay Miner.*, 49 (4), 559–568.

[26] Fatimah, I., 2018, Preparation, characterization and physicochemical study of 3-amino propyl trimethoxy silane-modified kaolinite for Pb(II) adsorption, *J. King Saud Univ., Sci.*, 30 (2), 250–257.

[27] Pramono, E., Umam, K., Sagita, F., Saputra, O.A., Alfiansyah, R., Setyawati Dewi, R.S., Kadja, G.T.M., Ledyastuti, M., Wahyuningrum, D., and Radiman, C.L., 2023, The enhancement of dye filtration performance and antifouling properties in amino-functionalized bentonite/polyvinylidene fluoride mixed matrix membranes, *Heliyon*, 9 (1), e12823.

[28] Yang, L., Qiu, J., Zhu, K., Ji, H., Zhao, Q., Shen, M., and Zeng, S., 2018, Effect of rolling temperature on the microstructure and electric properties of β-polyvinylidene fluoride films, *J. Mater. Sci.: Mater. Electron.*, 29 (18), 15957–15965.

[29] Yuliwati, E., Ismail, A.F., Matsuura, T., Kassim, M.A., and Abdullah, M.S., 2011, Characterization of surface-modified porous PVDF hollow fibers for refinery wastewater treatment using microscopic observation, *Desalination*, 283, 206–213.

[30] Stevenson, F.J., 1994, *Humus Chemistry: Genesis, Composition, Reactions*, 2nd Ed., John Wiley & Sons, New York.

[31] Teoh, G.H., Ooi, B.S., Jawad, Z.A., and Low, S.C., 2021, Impacts of PVDF polymorphism and surface printing micro-roughness on superhydrophobic membrane to desalinate high saline water, *J. Environ. Chem. Eng.*, 9 (4), 105418.

[32] Park, M.J., Wang, C., Seo, D.H., Gonzales, R.R., Matsuyama, H., and Shon, H.K., 2021, Inkjet printed single walled carbon nanotube as an interlayer for high performance thin film composite nanofiltration membrane, *J. Membr. Sci.*, 620, 118901.

[33] Zahid, M., Rashid, A., Akram, S., Rehan, Z.A., and Razzaq, W., 2018, A comprehensive review on polymeric nano-composite membranes for water treatment, *J. Membr. Sci. Technol.*, 8 (1), 1000179.

[34] Pramono, E., Alfiansyah, R., Ahdiat, M., Wahyuningrum, D., and Radiman, C.L., 2019, Hydrophilic poly(vinylidene fluoride)/bentonite hybrid membranes for microfiltration of dyes, *Mater. Res. Express*, 6, 105376.

[35] Marino, T., Russo, F., and Figoli, A., 2018, The formation of polyvinylidene fluoride membranes with tailored properties via vapour/non-solvent induced phase separation, *Membranes*, 8 (3), 71.

[36] Franco-Urquiza, E., Gamez Perez, J., Sánchez-Soto, M., Santana, O.O., and Maspoch, M.L., 2010, The effect of organo-modifier on the structure and properties of poly[ethylene–(vinyl alcohol)]/organo-modified montmorillonite composites, *Polym. Int.*, 59 (6), 778–786.

[37] Golz, E.K., and Vander Griend, D.A., 2013, Modeling methylene blue aggregation in acidic solution to the limits of factor analysis, *Anal. Chem.*, 85 (2), 1240–1246.

[38] Gayathri, S., and Govindaraju, K.M., 2019, Fabrication and characterization of Al/ZnO blended polyvinylidene fluoride (PVDF) membrane via electrospun method, *Res. J. Pharm. Technol.*, 12 (2), 787–790.

[39] Woo, S.H., Kim, K.M., Park, J., and Min, B.R., 2015, Preparation and characterization of poly(vinylidene fluoride) (PVDF) membrane, *Chem. Lett.*, 44 (1), 85–87.

[40] Fu, X., Zhu, L., Liang, S., Jin, Y., and Yang, S., 2020, Sulfonated poly(α,β,β-trifluorostyrene)-doped PVDF ultrafiltration membrane with enhanced hydrophilicity and antifouling property, *J. Membr. Sci.*, 603, 118046.

[41] Zhang, Y., Ye, L., Zhao, W., Chen, L., Zhang, M., Yang, G., and Zhang, H., 2020, Antifouling mechanism of the additive-free β-PVDF membrane in water purification process: Relating the surface electron donor monopolarity to membrane-foulant interactions, *J. Membr. Sci.*, 601, 117873.

[42] Mouri, E., Kajiwara, K., Kawasaki, S., Shimizu, Y., Bando, H., Sakai, H., and Nakato, T., 2022, Impacts of negatively charged colloidal clay particles on photoisomerization of both anionic and cationic azobenzene molecules, *RSC Adv.*, 12 (17), 10855–10861.

[43] Zhang, R., Liu, Y., Li, Y., Han, Q., Zhang, T., Zeng, K., and Zhao, C., 2020, Polyvinylidene fluoride membrane modified by tea polyphenol for dye removal, *J. Mater. Sci.*, 55 (1), 389–403.

[44] Liu, Y., Shen, L., Lin, H., Yu, W., Xu, Y., Li, R., Sun, T., and He, Y., 2020, A novel strategy based on magnetic field assisted preparation of magnetic and photocatalytic membranes with improved performance, *J. Membr. Sci.*, 612, 118378.

[45] Liu, X., Chen, Y., Deng, Z., and Yang, Y., 2020, High-performance nanofiltration membrane for dyes removal: Blending Fe_3O_4-HNTs nanocomposites into poly(vinylidene fluoride) matrix, *J. Dispersion Sci. Technol.*, 42 (1), 93–102.

[46] Zhao, Y., Yu, W., Li, R., Xu, Y., Liu, Y., Sun, T., Shen, L., and Lin, H., 2019, Electric field endowing the conductive polyvinylidene fluoride (PVDF)-graphene oxide (GO)-nickel (Ni) membrane with high-efficient performance for dye wastewater treatment, *Appl. Surf. Sci.*, 483, 1006–1016.